Short Papers

Electrostatic Potential Due to a Potential Drop Across a Slit

Young C. Noh and Hyo J. Eom

***Abstract*— The electrostatic potential and charge density due to a potential drop across a slit in a thick conducting plane are obtained in analytic closed form. The Fourier transform, mode matching, and superposition are used to represent the potential in the spectral domain. The residue calculus is applied to represent the potential distribution in converging series form. Numerical computations are performed to illustrate the charge–density distribution through a slit.**

***Index Terms*—Electrostatic potential, Fourier transform, mode matching, slit.**

I. Introduction

A study of potential difference across a slit in a conducting plane is an important subject for narrow-slit aperture antenna applications. A potential distribution due to a potential drop across a thick slit was considered in [1] using the Schwarz–Christoffel transformation. The motivation of this paper is to consider the electrostatic potential and charge density through the slit when a potential drop is applied across the slit in a thick conducting plane. We use the Fourier transform, mode matching, and superposition to obtain a converging series solution. Note that the Fourier transform and mode-matching technique have been successfully used in the study of static potential distribution through a slit [2]. In Section II, we present the field analysis in the spectral domain, and a brief summary is given in the conclusion.

II. Field Analysis

Consider a slit with a thickness d and width $2a$ in a thick perfectly conducting plane, shown in Fig. 1. The right and left conducting planes are assumed to be at potentials V and 0, respectively. In regions I ($z>0$) and III ($z<-d$), the potentials take the forms

$$\Phi^{\mathrm{I}}(x,z)=\frac{1}{2\pi}\int_{-\infty}^{\infty}\tilde{\Phi}^{\mathrm{I}}(\zeta)e^{-|\zeta|z-i\zeta x}\,d\zeta \tag{1}$$

$$\Phi^{\mathrm{III}}(x,z)=\frac{1}{2\pi}\int_{-\infty}^{\infty}\tilde{\Phi}^{\mathrm{I}}(\zeta)e^{|\zeta|(z+d)-i\zeta x}\,d\zeta \tag{2}$$

where $\tilde{\Phi}^{\mathrm{I}}(\zeta)$ is a Fourier transform of $\Phi^{\mathrm{I}}(x,0)$ given by $\tilde{\Phi}^{\mathrm{I}}(\zeta)=\int_{-\infty}^{\infty}\Phi^{\mathrm{I}}(x,0)e^{i\zeta x}\,dx$. The use of $\tilde{\Phi}^{\mathrm{I}}(\zeta)$ in (1) and (2) implies that $\Phi^{\mathrm{I}}(x,0)=\Phi^{\mathrm{III}}(x,-d)$. It is convenient to separate the boundary-value problem in region II ($-a<x<a$, $-d<z<0$) of Fig. 1 into two different cases [(a) and (b)], as shown in Fig. 2(a) and (b), respectively. Using the technique of the separation of the variable, we represent the potential in case (a) as a linear combination of $\cosh[a_m(z+d/2)]\sin a_m(x+a)$. The solution to the boundary-value problem for case (b) is available in [3]. Using the superposition, the total potential in region II is given by a sum of the solutions to the boundary-value problems, i.e., cases (a) and (b):

Manuscript received March 25, 1997; revised October 13, 1997.

The authors are with the Department of Electrical Engineering, Korea Advanced Institute of Science and Technology, Yusung-gu, Taejon 305-701, Korea.

Publisher Item Identifier S 0018-9480(98)02732-X.

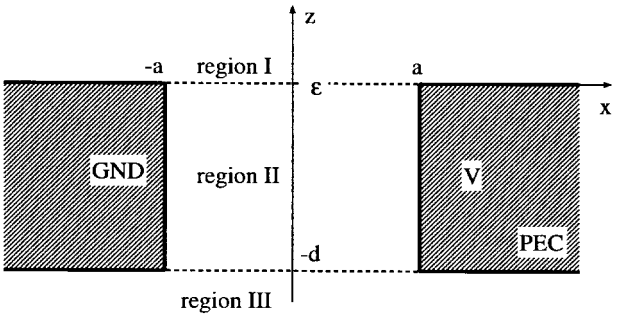

Fig. 1. Geometry of potential problem.

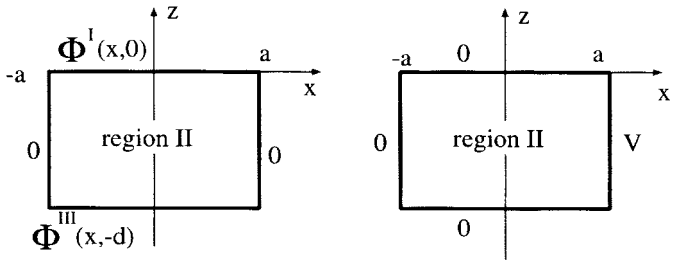

Fig. 2. Boundary conditions of region II.

$$\Phi^{II}(x,z)=\sum_{m=1}^{\infty}b_m\cosh\left[a_m\left(z+\frac{d}{2}\right)\right]\sin a_m(x+a)-\frac{4V}{\pi}\sum_{k=1}^{\infty}\frac{\sinh\dfrac{k\pi(x+a)}{d}}{k\sinh\dfrac{k\pi 2a}{d}}\sin\frac{k\pi z}{d} \tag{3}$$

where $a_m=m\pi/(2a)$, $m=1,2,3,\cdots$, and $k=1,3,5,\cdots$.

By symmetry of the boundary condition, we note $\Phi^{\mathrm{I}}(x,0)=\Phi^{\mathrm{III}}(x,-d)$ and $(\partial\Phi^{\mathrm{I}}(x,z)/\partial z)|_{z=0}=-(\partial\Phi^{\mathrm{III}}(x,z)/\partial z)|_{z=-d}$. This implies that we only need to enforce the boundary condition at $z=0$. The boundary conditions to be enforced are

$$\Phi^{\mathrm{I}}(x,0)=\begin{cases}0, & x<-a\\ \Phi^{\mathrm{II}}(x,0), & |x|<a\\ V, & x>a\end{cases} \tag{4}$$

$$\left.\frac{\partial\Phi^{\mathrm{I}}(x,z)}{\partial z}\right|_{z=0}=\left.\frac{\partial\Phi^{\mathrm{II}}(x,z)}{\partial z}\right|_{z=0},\qquad |x|<a. \tag{5}$$

Applying the Fourier transform to (4), we obtain

$$\tilde{\Phi}^{\mathrm{I}}(\zeta)=\int_{-a}^{a}\Phi^{\mathrm{II}}(x,0)e^{i\zeta x}\,dx+V\int_{a}^{\infty}e^{i\zeta x}\,dx. \tag{6}$$

Substituting (3) into (6), and performing integration

$$\tilde{\Phi}^{\mathrm{I}}(\zeta)=\sum_{m=1}^{\infty}b_m\cosh\frac{a_m d}{2}F_m(\zeta)+Ve^{i\zeta a}\left[\pi\delta(\zeta)-\frac{1}{i\zeta}\right] \tag{7}$$

where $\delta(\zeta)$ is the Dirac delta and $F_m(\zeta)=a_m[(-1)^m e^{i\zeta a}-e^{-i\zeta a}]/\zeta^2-a_m^2$. Substituting $\Phi^{\mathrm{I}}(x,z)$ of (1) into (5), multiplying

(5) by $\sin a_n(x+a)$, and integrating, with respect to x, from $-a$ to a, we obtain

$$-\frac{1}{2\pi}\int_{-\infty}^{\infty}\tilde{\Phi}^{\mathrm{I}}(\zeta)|\zeta|F_n(-\zeta)\,d\zeta = aa_nb_n\sinh\frac{a_nd}{2}+\frac{4V}{d}\sum_{k=1}^{\infty}\frac{a_n\cos n\pi}{(k\pi/d)^2+a_n^2}. \quad (8)$$

Substituting (7) into (8), we obtain

$$-\sum_{m=1}^{\infty}b_m\cosh\frac{a_md}{2}\frac{1}{2\pi}\int_{-\infty}^{\infty}|\zeta|F_m(\zeta)F_n(-\zeta)\,d\zeta - (-1)^n\left[\frac{V}{2}+\frac{V}{\pi}\,\mathrm{si}(n\pi)\right] = aa_nb_n\sinh\frac{a_nd}{2} + \frac{4V}{d}\sum_{k=1}^{\infty}\frac{a_n\cos n\pi}{(k\pi/d)^2+a_n^2}. \quad (9)$$

It is shown in [2] that

$$\frac{1}{2\pi}\int_{-\infty}^{\infty}|\zeta|F_m(\zeta)F_n(-\zeta)\,d\zeta = aa_n\delta_{nm}-J_{nm} \quad (10)$$

where δ_{nm} is the Kronecker delta and

$$J_{nm}=\begin{cases}0, & m+n=\text{odd}\\ \dfrac{2a_na_m}{\pi(a_n^2-a_m^2)}\left[\ln\left(\dfrac{a_n}{a_m}\right)+\mathrm{ci}(m\pi)-\mathrm{ci}(n\pi)\right], & m+n=\text{even}\\ \dfrac{a_m}{\pi a_n}[2-(n\pi)\,\mathrm{si}(n\pi)], & m=n\end{cases} \quad (11)$$

$\mathrm{ci}(\cdot)$ and $\mathrm{si}(\cdot)$ are the cosine and sine integrals, respectively. Substituting (10) into (9), we get

$$B=\Psi^{-1}\Gamma \quad (12)$$

where B and Γ are column vectors of b_n and γ_n

$$\psi_{nm}=\delta_{nm}-\frac{e^{(a_m-a_n)d/2}+e^{-(a_m+a_n)d/2}}{2aa_n}J_{nm} \quad (13)$$

$$\gamma_n=(-1)^{n+1}\frac{e^{-a_nd/2}}{aa_n}\left[\frac{V}{2}+\frac{V}{\pi}\,\mathrm{si}(n\pi)+\frac{4V}{d}\sum_{k=1}^{\infty}\frac{a_n}{(k\pi/d)^2+a_n^2}\right]. \quad (14)$$

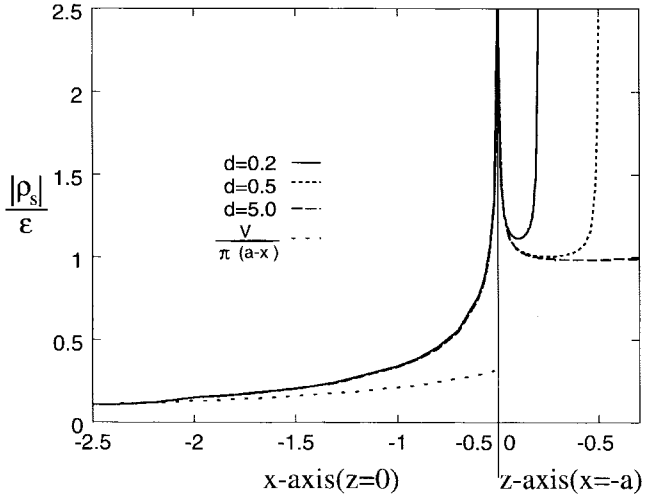

Fig. 3. Charge–density distribution.

Substituting (7) into (1) and performing the contour integration with respect to ζ, we obtain $\Phi^{\mathrm{I}}(x,z)$ in convergent series forms (15)-(17), shown at the bottom of the page, where $\mathrm{Im}[\cdot]$ is the imaginary part of $[\cdot]$ and$K(\beta,\mu)=(1/\beta)\,[\mathrm{ci}(\beta\mu)\sin(\beta\mu)-\mathrm{si}(\beta\mu)\cos(\beta\mu)]$. Equations (3) and (15)–(17) constitute converging series solutions for the potential distribution through a thick slit. From (1) to (3), we obtain the charge–density distribution on the conducting surface, shown in (18), at the bottom of the page, where $P(\beta,\mu)=\mathrm{ci}$, $(\beta\mu)\cos(\beta\mu)+\mathrm{si}$, $(\beta\mu)\sin(\beta\mu)$, and ϵ is the permittivity. Fig. 3 shows the behavior of the charge density $|\rho_s|/\epsilon$ on the conducting surface when $a=0.5$ and $V=1$. We use $m=31$ in (18) to achieve the numerical accuracy within 1% error. As d/a increases, the convergence rate of (18) becomes better. It is seen that $|\rho_s(x,0)|/\epsilon$ remains almost unchanged as d varies. When $x<-2$, $|\rho_s(x,0)|/\epsilon$ almost approaches $V/\pi(a-x)$, implying an influence from the charge near the slit is negligible. When d is rather large (i.e., $d=5$), $|\rho_s(-a,z)|/\epsilon\simeq 1$ except near a singular point at $z=0$. Note that $|\rho_s(-a,z)|/\epsilon=1$ for an infinitely thick slit $(d=\infty)$.

III. Conclusion

The potential distribution due to a potential drop across a slit is solved with the Fourier transform, mode matching, and superposi-

$$\Phi^{\mathrm{I}}(x,z)=\sum_{m=1}^{\infty}\frac{a_mb_m}{\pi}\cosh\frac{a_md}{2}\cdot\mathrm{Im}\{(-1)^mK[a_m,a-x+iz]-K[a_m,-(a+x)+iz]\}+\frac{V}{2}-\frac{V}{\pi}\arctan\left(\frac{a-x}{z}\right),\qquad x<-a \quad (15)$$

$$=\sum_{m=1}^{\infty}\frac{a_mb_m}{\pi}\cosh\frac{a_md}{2}\cdot\mathrm{Im}\{(-1)^mK[a_m,a-x+iz]-K[a_m,a+x+iz]\}+b_m\cosh\frac{a_md}{2}e^{-a_mz}\sin a_m(a+x)+\frac{V}{2}-\frac{V}{\pi}\arctan\left(\frac{a-x}{z}\right),\qquad |x|\le a \quad (16)$$

$$=\sum_{m=1}^{\infty}\frac{a_mb_m}{\pi}\cosh\frac{a_md}{2}\cdot\mathrm{Im}\{(-1)^mK[a_m,x-a+iz]-K[a_m,a+x+iz]\}+\frac{V}{2}+\frac{V}{\pi}\arctan\left(\frac{x-a}{z}\right),\qquad x>a \quad (17)$$

$$\frac{|\rho_s(x,z)|}{\epsilon}=\begin{cases}\displaystyle\sum_{m=1}^{\infty}\frac{a_mb_m}{\pi}\cosh\left(a_m\frac{d}{2}\right)[(-1)^mP(a_m,a-x)-P(a_m,-a-x)]+\frac{V}{\pi}\frac{1}{a-x}, & x<-a,z=0\\ \displaystyle\sum_{m=1}^{\infty}a_mb_m\cosh\left[a_m\left(z+\frac{d}{2}\right)\right]-\frac{4V}{d}\sum_{k=1,3}^{\infty}\frac{\sin\dfrac{k\pi z}{d}}{\sinh\dfrac{k\pi 2a}{d}}, & \dfrac{-d}{2}<z<0,x=-a\end{cases} \quad (18)$$

tion. The solutions are represented in convergent series form, and numerical computations are performed to show the charge–density distribution through the slit.

REFERENCES

[1] L. K. Warne and K. C. Chen, "Relation between equivalent antenna radius and transverse line dipole moments of a narrow slit aperture having depth," *IEEE Trans. Electromagn. Compat.*, vol. 30, pp. 364–370, Aug. 1988.
[2] Y. S. Kim and H. J. Eom, "Fourier-transform analysis of electrostatic potential distribution through a thick slit," *IEEE Trans. Electromagn. Compat.*, vol. 38, pp. 77–79, Feb. 1996.
[3] D. W. Trim, *Applied Partial Differential Equations.* Boston, MA: PWS, 1990, pp. 115–117.

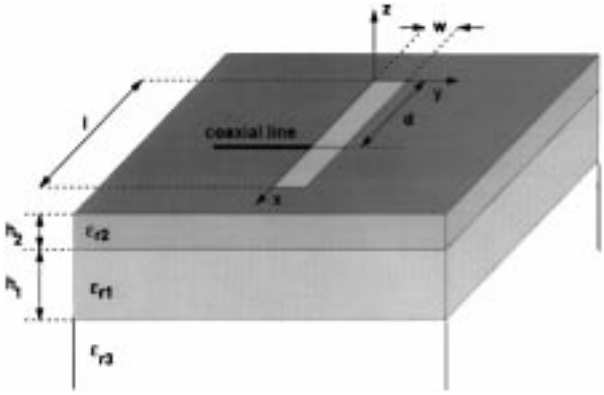

Fig. 1. A slot structure on a multilayer medium. The region above the slot is free space.

A Numerically Efficient Technique for the Analysis of Slots in Multilayer Media

Noyan Kınayman, Gülbin Dural, and M. I. Aksun

***Abstract*— A numerically efficient technique for the analysis of slot geometries in multilayer media is presented using closed-form Green's functions in spatial domain in conjunction with the method of moments (MoM). The slot is represented by an equivalent magnetic-current distribution, which is then used to determine the total power crossing through the slot and the input impedance. In order to calculate power and current distribution, spatial-domain closed-form Green's functions are expanded as power series of the radial distance ρ, which makes the analytical evaluation of the spatial-domain integrals possible, saving a considerable amount of computation time.**

***Index Terms*—Green's function, moment methods, multilayers.**

I. INTRODUCTION

Slot geometries have a broad spectrum of applications either as transmission lines or radiating elements, and have been examined extensively in the literature [1]–[4]. The most commonly used numerical technique for analyzing the slot geometries is the method of moments (MoM), which can be applied in either the spatial or spectral domains. Although the MoM is preferred over the differential equation methods because it is relatively efficient in terms of the computation time, it is still time consuming because of the slow convergence and the oscillatory nature of the integrals involved. One approach to overcome these difficulties is to employ the closed-form Green's functions in the spatial domain, which can speed up the computation of the MoM matrix elements by several orders of magnitude as compared to the numerical evaluation of the Sommerfeld integral [5]–[8].

In this paper, the Galerkin's MoM analysis of the slot geometries in multilayer media has been developed by employing the closed-form Green's functions for the vector and scalar potentials of a horizontal magnetic dipole (HMD) in the spatial domain [9]. The formulation is presented for narrow slot geometries excited with coaxial-line feed; however, it can be applied to slot geometries of any kind of excitation without any major modification. The equivalent magnetic-current distribution of the slot is computed and used for the computation of power crossing the slot and the input impedance. Numerical calculation of power crossing the slot and the equivalent magnetic slot current is computationally a very demanding procedure because the numerical evaluation of the integrals involved is very time consuming in either the spatial or spectral domains. Here, the spatial-domain Green's functions are approximated as a power series of radial distance ρ, and integrals involving the Green's functions are carried out analytically, saving a considerable amount of computational time both in current and power calculations [10].

Manuscript received August 22, 1996; revised January 14, 1998. This work was supported in part by NATO's Scientific Affairs Division in the framework of the Science for Stability Programme.

N. Kınayman and M. I. Aksun are with the Department of Electrical and Electronics Engineering, Bilkent University, 06533 Ankara, Turkey.
G. Dural is with the Department of Electrical and Electronics Engineering, Middle East Technical University, 06531 Ankara, Turkey.

Publisher Item Identifier S 0018-9480(98)02733-1.

II. FORMULATION

An example of a narrow slot placed in a multilayer medium is shown in Fig. 1. It is assumed that the layers extend to infinity in the transverse direction and the slot is excited with a coaxial line of current I_{in} amperes at the feeding point. It is also assumed that there is no conducting or dielectric losses. Therefore, the only loss mechanism is the radiation.

The tangential component of the magnetic field on the slot can be expressed in terms of an equivalent magnetic-current density $\vec{J}^m$ using the mixed-potential integral equation (MPIE) formulation [11] as follows:

$$H_x = -j\omega G_{xx}^F * J_x^m + \frac{1}{j\omega}\frac{\partial}{\partial x}(G_x^{qm} * \nabla \cdot \vec{J}^m) \tag{1}$$

where J_x^m is the longitudinal component of the current density $\vec{J}^m$, and G_{xx}^F and G_x^{qm} are the spatial-domain Green's functions for the vector and scalar magnetic potentials for an HMD, respectively. To solve for the equivalent magnetic current density J_x^m using the MoM, the current density is expressed as a linear combination of suitable subdomain basis functions in the following form:

$$J_x^m = \sum_{n=1}^{N} I_{xn} B_{xn}(x,y) \tag{2}$$

where B_{xn}'s are the basis functions which are chosen in this paper to be rooftops. Since a narrow slot is assumed, the current variation in y-direction is considered to be constant. Enforcing the boundary